

Updated Kinetic Mechanism for NO_x Prediction and Hydrogen Combustion

Milestone M2.2

SEVENTH FRAMEWORK PROGRAMME

FP7-ENERGY-2008-TREN-1

ENERGY-2008-6-CLEAN COAL TECHNOLOGIES

Project Acronym: H2-IGCC

Project Full Title: Low Emission Gas Turbine Technology for Hydrogen-rich Syngas

Grant Agreement No.: 239349

SP1: Combustion



Mayuri Goswami
Evgeniy N. Volkov
Alexander A. Konnov
R.J.M. Bastiaans
L.P.H. de Goey

Department of Mechanical Engineering
Technische Universiteit Eindhoven
Eindhoven, The Netherlands

Abstract

An updated kinetic mechanism of H_2/O_2 system along with NO_x prediction mechanism has been presented on the basis of an extensive literature survey of new experimental data. The most recent mechanisms have been used for analyzing the reactions and comparisons. The main focus of the present work is to investigate the effect of high pressure (upto 20 atm) at lean (equivalence ratio, $\phi < 0.8$) premixed combustion mode. The proposed mechanism takes into consideration the complexities of higher pressure. Simulations using mechanisms by Rasmussen et al. [1], Frassoldati et al. [9], GRI mech 3.0 [2] have been carried out and compared with the present updated mechanism. The mechanism by Rasmussen et al. [1] has also been performing well under these conditions. At conditions of high N_2 in the oxidizer mixture (O_2/N_2) when the flame temperatures are low, present mechanism and that by Frassoldati et al. [9] perform better. GRI mech 3.0 [2] on the other hand, performed unsatisfactorily for pure Hydrogen/air lean mixtures even at atmospheric pressure including prediction of NO_x .

Introduction

The application of hydrogen as a fuel in technologies like IGCC systems has been of great interest to researchers around the world. Usage of high hydrogen content fuel not only reduces production of certain pollutants, it also increases the scope of utilizing its high energy content in the form of a fuel. Hydrogen exhibits high reactivity and large flame speeds. High hydrogen content in combination with other gases like CO_2 and CH_4 is the present trend of syngas that requires great deal of research. The above mentioned technology aims at using such fuels in a lean combustion mode at high pressure and temperature. The design and development of gas turbine combustors used for such combustion systems is based more on detailed computer models and thus requires deep knowledge of kinetics of these gases. A kinetic mechanism has an important role in the development of this kind of advanced combustion technology that aims at the combustion of hydrogen rich syngas fuel. Simulation of the reacting flows is the basis for designing the combustors. The kinetic mechanism is one of the key tools in predicting characteristics like flame speed, ignition delay, autoignition and flashback for implementation in commercial CFD codes. Hence, it is of utmost importance to analyze the kinetics of each reaction, their behavior at different conditions of pressure, temperature and fuel/oxidizer composition and implication on the formation of pollutants.

Hydrogen in itself possesses complex chemistry at gas turbine conditions and also pertinent reactions find its place in hydrocarbon combustion chemistry. High adiabatic temperature involved with above systems also favors thermal NO_x formation. Very high flow rates of cost-intensive dilution gases like N_2 and H_2O are needed to combust syngas in highly-diluted diffusion flames and to control NO_x emissions. Current technology is not yet designed for hydrogen-rich syngas in low NO_x premix systems. Hence, to modify existing burner technology to operate on hydrogen-rich syngas in lean premixed combustion mode (undiluted) fuel chemistry is of high importance.

The present work gives a review of recent mechanisms and an updated list of rate constants for the reactions relevant for H_2 reacting systems and prediction of NO_x at conditions that are relevant to gas turbine combustion. This report includes a section reviewing important H_2/NO_x mechanisms that emerged in last few years. Comparisons of these mechanisms with various experimental results have also been highlighted. The following section describes certain possible routes of NO formation with such kind of mixtures. The next section includes a description of the rate constants that have been used in the updated mechanism. The final section is dedicated in comparing these mechanisms with experimental data which includes laminar burning velocity, ignition delay, NO concentration comparisons.

Review of Recent Models

H/O mechanisms

One of the most important mechanisms for H₂/O₂ systems in the past decade was Mueller's mechanism [3]. It was conceived as a part of modeling of their flow reactor experiments ranging from 0.3 to 15.7 atm and 850-1040K. Many of the rate constants recommended by them were from Tsang and Hampson[4]. Aung et al.[5,6] performed experiments on freely propagating spherical laminar premixed flames to study the effects of pressure and nitrogen dilution on flame stretch. They compared their measurements with detailed mechanisms by Kim et al. [7], Wang and Rogg[8] and GRImech 2.1 [2], till date these data are being used for comparisons [9]. Tse et al. [10] designed another experimental setup that measured burning rates of H₂/O₂/inert mixtures upto 60 atm. Comparisons were done with the measured values by Aung et al.[6] and Taylor [11] in addition to simulations of Mueller et al. [3]. Also, they observed cell formation over the flame surface due to hydrodynamic and diffusive-thermal instabilities and that wrinkled flame is the dominant mode of propagation of H₂/air flames at high pressures. Using Helium as a diluent, these effects were suppressed. Kwon and Faeth [12] investigated flame/stretch interactions of mixtures of H₂, O₂, N₂, Ar and He at equivalence ratio varying from 0.6 to 4.5 with pressures from 0.3 to 3.0 atm. Wang et al. [13] studied ignition delay times from their heated shock tube experiments of H₂-air steam mixtures for various pressures, temperatures and fuel compositions. The experimental results were then compared with simulations with the Grimech 2.1, 3.0[2], models by Baulch et al. [14], Allen et. Al. [15], Konnov [16] and Miller and Bowman[17]. The mechanism by Li et al. [18,19] for H₂ combustion has been good at atmospheric and high pressure conditions and has been under constant research limelight. This mechanism at the time of its publication was compared with the then existing mechanism by Mueller et al.[3].

H/N/O mechanisms

Skottene and Rian [20] and Strohle and Myhrvold [21,22] carried out comparison on NO_x formation in H₂/air flames and H₂ combustion at gas turbine conditions respectively and recommended Li et al. mechanism[19]. Frassoldati et al. [9,44] presented another updated mechanism with comparison with wide range of modeling and experimental studies which included premixed, counterflow diffusion flames, ammonia chemistry and reactor studies. They performed numerical simulations of combustion of hydrocarbons, hydrogen to predict NO_x and compared with a variety of experimental results from literature. Their updated mechanism in 2006 looked specifically into reactions like



More recently for syngas and gas turbine technology studies mechanisms by Davis et al. [23] , Saxena and Williams [24] and Sun et al. [25] for H₂/CO mixtures for high pressure conditions have emerged. Comparisons of these mechanisms have been done with flow reactor concentration profiles and shock tube ignition delay experiments. Rasmussen et al. [1] performed high pressure flow reactor experiments on H₂/O₂/CO/NO_x mixtures and presented updated chemistry set for pressures of 20-100 bars and temperatures of 600-900 K. They also updated a few rate constants of the H/N/O chemistry using ab initio calculations. Another updated kinetic mechanism by Konnov [26]

has been presented with analysis of certain species like OH and HO₂ and pressure dependence of reactions. Predictions of ignition, oxidation, flame burning velocities and flame structure of H₂-O₂-inert mixtures were shown. Burke et al. [27] have discussed the sources of uncertainties in a number of reactions in H₂-O₂ mechanism that are pressure dependent under lean and rich conditions as they realized substantial difference between literature model predictions and experimental data.

Glarborg et al. [28,29] introduced a hydrocarbon/NO_x mechanism which was compared to their quartz flow reactor experimental results. Konnov et al. [30] through their numerical simulations and comparisons for well stirred reactors for lean and rich H₂/air mixtures in the temperature range 1500-2000K, presented an updated H/N/O mechanism. The rate constant of the reaction



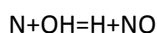
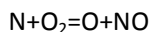
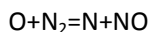
was derived keeping in view its temperature dependence by comparing experiments at low pressure H₂/air at 1200 K thereby updating the detailed H/N/O kinetic mechanism. A final tuning of the same reaction was done by the same group [31] using the experimental results of Xie et al.[32] and Harrington et al.[33]. Konnov and De Ruyck [34,35] developed the N/H subset of the kinetic mechanism by studying the thermal decomposition of ammonia and hydrazine. This study reproduced results for low and atmospheric pressure. NO formation in stirred reactors by the same group [36] was done which was compared with the experimental results of Engleman et al. [37]. This work also threw light on a possible new route for NO formation via N₂H₃. Konnov [38] through his study over H₂/O₂/N₂ flames concluded that for lean combustion both thermal NO and NNH routes could be equally important, the latter route being dominant below 2000 K. Numerical studies by Skottene and Rian[20] suggested that for hydrogen combustion the Li et al. mechanism[18] for the H₂ subset and NO_x subset from Glarborg et al.[29] gives convincing results. They also concluded that the San Diego mechanism [39] omits the important NO forming pathway NNH+O=NO+NH proposed in [40]. Xu and Lin [41-43] suggested new rate constants by ab initio calculations for the pressure dependent reactions:



A detailed N/O kinetic mechanism was developed by Konnov and De Ruyck[45] which is further updated by Volkov et al. [46] in comparison with experimental data for N₂O ignition, NO and NO₂ decomposition at high temperatures. This mechanism performed satisfactorily except in predicting burning velocities of pure N₂O. Studies of NO or NH₃ doped H₂/O₂/N₂ flames were done by Shmakov et al.[47] at atmospheric pressure. They recommended replacement of reaction NH+H₂O=HNO+H₂ with NH+H₂O=NH₂OH as it brought improvement in their model for rich mixtures. This change has been implemented in the present proposed updated model also. There have been extensive review of rate constants of a number of reactions performed by Baulch et al. [14,48,49]. Many of the rate constants suggested by the above mentioned mechanisms are a result of this review. The present mechanism also uses many of these rate constants.

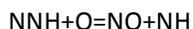
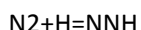
Routes of NO formation

Thermal NO_x or extended Zeldovich mechanism is one of the key mechanisms through which NO_x formation chemistry is understood. But, there exists other routes too for NO_x production that may be resultant of other conditions like lean or rich nature of the mixture or high pressure. Thermal NO is significant at temperatures above 1700K. The following three reactions depict the formation of thermal NO:



At high temperatures ($T > 1700\text{K}$) diatomic nitrogen and oxygen dissociate into their atomic states, participating in a series of reactions thereby forming NO as given above.

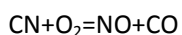
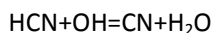
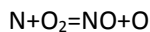
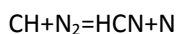
Via NNH also a route has been suggested as depicted by the following reactions:



Reaction of NNH with O has the following channels: $\text{NH} + \text{NO}$, $\text{N}_2\text{O} + \text{H}$ and $\text{N}_2 + \text{OH}$. The first channel is a route of NO formation via NNH and was first reported by Bozzelli and Dean[41] in 1995. The rate constant calculated by them was $k = 3.3 \times 10^{14} T^{0.23} \exp(+510/T) \text{ cm}^3 \text{ mol}^{-1} \text{ s}^{-1}$. Evaluation of this route shows that this pathway is important at low residence times for high temperature (2200 K), except for lean mixtures. At temperatures upto 1900K NNH-pathway is important for all residence times with most pronounced at stoichiometric, low temperature condition. The kinetic significance of NNH was first suggested by Miller et al.[51] which was a basis to the emergence of the study of this route.

Via N₂H₃, Konnov and Ruyck [36] suggested formation of NO if a pathway is found to form N₂H₃. Molecular nitrogen reacts with H to form NNH, which in subsequent reactions with H forms N₂H₂ and then N₂H₃. This species is reduced by H₂ to NH₃ and NH₂. Further, these species can be oxidized in the sequence $\text{NH}_3 \rightarrow \text{NH}_2 \rightarrow \text{NH} \rightarrow \text{N} \rightarrow \text{NO}$. This route was later adopted in all major mechanisms.

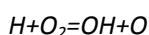
Prompt NO_x mechanism results from N₂ being in contact with radicals like C, CH and CH₂ where they react to species containing N and getting further oxidized to NO. Two such channels are shown below.



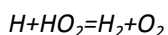
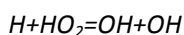
The present study does not involve the chemistry of carbon containing reactants and hence prompt mechanism is not discussed in this work.

Reaction Mechanism and Choice of Rate Constants

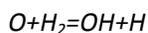
Selected reactions with updated rate constants from an extensive literature survey are presented in Table 1. The mechanism deals with H/N/O containing species, with 32 species and 237 reactions. The hydrogen sub-mechanism is an updated version of the mechanism published by Konnov [26]. In the recent study of Burke et al. [27], many mechanisms [19, 23-26, 50] were observed to have discrepancies when compared to experiments and among model predictions themselves. Since this study was performed for a wide range of flame temperatures, pressures and equivalence ratios, the above mechanisms could not perform well at all conditions. With an update in Konnov [26], the present mechanism is believed to work better at lean high pressure (upto 20 bar) conditions.



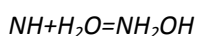
This reaction (9) signifies chain branching and the production of OH radical which are of importance to hydrogen combustion and NO_x chemistry. Various experiments have been performed to determine the rate constant of this reaction but only at temperatures greater than 500 K. Literature data [52] suggests that still disagreement prevails in their determination. Low temperature experiments have not been possible resulting in prohibition of consistent results over a sufficient wide temperature range. Baulch et al. [49] reviewed data from a number of sources mostly shock tube experiments for pressure up to 4 bar. In the review, experiments and simulation results of Hwang et al. [52] the rate constant finds a non-Arrhenius expression defined for a temperature range of 950-3100 K. Also, in this reaction, as per the calculations of Troe and Ushakov [53], a back reaction has negative temperature dependence (at T>500 K) which is well supported by the constant derived by Hwang et al.[52]. The present mechanism uses their expression of the rate constant.



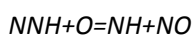
For lower temperatures a number of reasonable data is available and hence evaluations of rate constants for these reactions (13,15) have been accepted. However, at higher temperatures the data is scarce. Mueller and Yetter [3] performed flow reactor studies and determined the rate constants of the above reactions for a range of temperatures and pressures. They inferred with a compilation of data into a summarized figure depicting kinetic response of the H₂/O₂/N₂ mixture to changes of pressure (upto 100 atm) and stoichiometry with new explosion limit data. As per their conclusions the reaction HO₂+H=H₂+O₂ shows high sensitivity towards lean conditions and is more important than the other competing reaction. The third possible route HO₂+H=H₂O+O has not been included in the present study as well as many previous studies due to its large uncertainty in the rate constant due to its slow nature. The rate constants recommended by Mueller and Yetter [3] have been included in the present mechanism.



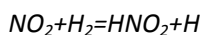
The rate constant of this reaction (8) has been reviewed a number of times and have been of great experimental interest. Due to its variation at high and low temperature and also of high significance in hydrogen chemistry, the rate constant finds good importance in the hydrogen mechanism. This reaction is one of the pathways to the formation of OH that in turn gives a path to NO formation through thermal NO_x mechanism. In the work of Baulch et al. [49], a review has been performed ever since 1972 including Cohen and Westberg [54] and Tsang and Hampson[55]. The mechanism of Konnov[26] adopted rate constant derived by Sutherland et al. [56] which extrapolates even to high temperatures [1700-3500K]. In the present mechanism a slightly improved value of Baulch et al. [49] is adopted that also fits low temperature data.



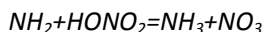
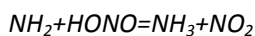
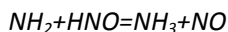
The basic structure of H/N/O sub-mechanism of the present model comes from Coppen et al. [57] and Konnov 0.5 version[16]. The update of this set is described in the subsequent paragraphs. Shmakov et al. [47] performed experiments on H₂+O₂+N₂ flames doped with NO or NH₃ at atmospheric pressure and reviewed the role of the reaction NH+H₂O=HNO+H₂ in the post flame zone of lean and stoichiometric flames. Glarborg and coworkers [1] ruled out including this reaction as it was slow. But further experimental studies supported the rate constants of Rohrig and Wagner[58] which is also included in the present model and also GRImech3.0, however with the proposal of using NH₂OH as the possible product of the reaction. Hence, it was recommended to replace NH+H₂O=HNO+H₂ by NH+H₂O=NH₂OH [47] represented by reaction 187. This change has a small effect on lean and stoichiometric flames, but significant improvement in the prediction of rich flames on spatial profiles of NO and NH₃.



As reported above, this reaction (189) is considered another route to the formation of NO. Harrington et al. [33] through their experiments recommended this route of NO formation as there were no sources of thermal NO_x or prompt NO_x in their experiments. Previous studies [59] have showed that this route of NO formation is of major importance in hydrogen combustion in a stirred reactor, even for lean mixtures at 1400-1560 K. Konnov and De Ruyck [60] derived a rate constant for this reaction by comparing experiments in low pressure(0.05 and 0.103 bar) hydrogen-air flames at 1200 K. The derived rate constant was further tuned to $k=1\pm 0.5E14 \exp(-16.75\pm 4.2 \text{ KJ/mol/RT}) \text{ cm}^3\text{mol}^{-1}\text{s}^{-1}$ by Konnov et al. [31] bringing modeling closer to experimental results for stoichiometric and lean flames. The present mechanism incorporates the above tuned value of the rate constant.



The above reaction (123) is insignificant at temperatures less than 1600K but has quite high product yield at temperatures higher than that. Rate constant suggested by Rasmussen et al.[1] is an outcome of their ab initio calculations and those by Park et al.[61]. This value is incorporated in the present mechanism.



The above reactions (141,153,160) are highly important in the study of ammonia flames and deNO_x processes. Glarborg and coworkers [28,62] have experimentally studied the NH₃-NO_x system and suggested a rate constant but without temperature dependence. The rate constants of the above reactions have been studied and published most recently by Xu and Lin[41-43] by performing ab initio calculations. These are major reactions in the production of NO_x species especially active at high pressure via N₂H₃ route [36]. The recommended values of the rate constants are valid for a temperature range of 200-3000 K. Reaction NH₂+HNO=NH₃+NO has pressure dependence at T < 600 K from pressure 1 Torr to 100 atm due to a rate constant which decreases with increasing temperature from 300 to 3000 K. Reaction NH₂+HONO=NH₃+NO₂ shows no pressure dependence. On the other hand, reaction NH₂+HNO₃=NH₃+NO₃ shows noticeable pressure dependence at T < 900 K. This reaction has not been included in many NO_x mechanism including latest version of Konnov [16] and Rasmussen et al. [1]. The rate constants suggested by Xu and Lin have been adopted in the present mechanism.

N/O chemistry

The kinetic modeling study performed by Konnov and De Ruyck [45] includes the basic mechanism for N/O chemistry which is most recently updated by Volkov et al.[46] and has been included in the present mechanism. Both these studies have been performed for NO_x decompositions at flame temperatures and included around 29 reactions. Without any adjustment of the rate constants the proposed N/O kinetic mechanism allows at least satisfactory reproducing widely differing sets of experimental data on NO_x decomposition, obtained at initial concentrations of NO_x ranging from 0.1 to 100%, pressures ranging from 0.5 to 14 atm and temperatures ranging from 630 to 3850 K. Observed differences relate both to experimental uncertainty and uncertainty of our current knowledge of the rate constants of N/O reactions.

Table 1 : Reaction mechanism and Rate constants, $k=AT^n \exp(-E_A/RT)$, units : $\text{cm}^3\text{-mole-s-cal-K}$

nO	Reaction	A	n	E_A	Reference
1a	H+H+M=H ₂ +M Enhanced third-body efficiencies(relative to Ar) H ₂ =0, N ₂ =0, H=0, H ₂ O=14.3	7.00E+17	-1	0	[26]
1b	H+H+H ₂ =H ₂ +H ₂	1.00E+17	-0.6	0	[26]
1c	H+H+N ₂ =H ₂ +N ₂	5.40E+18	-1.3	0	[26]
1d	H+H+H=H ₂ +H	3.20E+15	0	0	[26]
2	O+O+M=O ₂ +M Enhanced third-body efficiencies(relative to Ar) O=28.8, O ₂ =8, N ₂ =2.0	1.00E+17	-1	0	[26]
3	O+H+M=OH+M Enhanced third-body efficiency: H ₂ O=5.0	6.75E+18	-1	0	[26]
4	H+OH+M=H ₂ O+M Enhanced third-body efficiencies(relative to N ₂) H ₂ O=6.4, Ar=0.38	2.20E+22	-2	0	[26]
5a	H ₂ O+M=H+OH+M Enhanced third-body efficiencies(relative to Ar) H ₂ O = 0, H ₂ = 3, N ₂ = 2, O ₂ = 1.5	6.06E+27	-3.312	120770	[26]
5b	H ₂ O+H ₂ O=H+OH+H ₂ O	1.00E+26	-2.44	120160	[26]
6a	H+O ₂ (+M)=HO ₂ (+M) Low pressure limit: F _{cent} =0.5 Enhanced third-body efficiencies(relative to N ₂) Ar=0, H ₂ O=0, O ₂ =0, H ₂ =1.5, He=0.57	4.66E+12 5.70E+19	0.44 -1.4	0 0	[26]
6b	H+O ₂ (+AR)=HO ₂ (+AR) Low pressure limit: F _{cent} =0.5	4.66E+12 7.43E+18	0.44 -1.2	0 0	[26]
6c	H+O ₂ (+O ₂)=HO ₂ (+O ₂) Low pressure limit: F _{cent} =0.5	4.66E+12 5.69E+18	0.44 -1.094	0 0	[26]
6d	H+O ₂ (+H ₂ O)=HO ₂ (+H ₂ O) Low pressure limit: F _{cent} =0.8	9.06E+12 3.67E+19	0.2 -1.0	0 0	[26]
7a	OH+OH(+M)=H ₂ O ₂ (+M) Low pressure limit: F _{cent} =0.5 Enhanced third-body efficiency H ₂ O=0	1.00E+14 2.38E+19	-0.37 -0.8	0 0	[26]
7b	OH+OH(+H ₂ O)=H ₂ O ₂ (+H ₂ O) Low pressure limit: F _{cent} =0.5	1.00E+14 1.45E+18	-0.37 0	0 0	[26]
8	O+H ₂ =OH+H	3.82E+12	0	7948	[49]
	O+H ₂ =OH+H	8.79E+14	0	19170	[49]
9	H+O ₂ =OH+O	6.73E+15	-0.5	16670	[52]
10	H ₂ +OH=H ₂ O+H	2.14E+08	1.52	3450	[26]
11	OH+OH=H ₂ O+O	3.34E+04	2.42	-1930	[26]
12	HO ₂ +O=OH+O ₂	1.63E+13	0	-445	[26]
13	H+HO ₂ =OH+OH	7.08E+13	0	295	[3]
14	H+HO ₂ =H ₂ O+O	1.45E+12	0	0	[26]
15	H+HO ₂ =H ₂ +O ₂	1.66E+13	0	823	[3]

16	$H_2+O_2=OH+OH$	2.04E+12	0.44	69155	[26]
17	$HO_2+OH=H_2O+O_2$	2.89E+13	0	-500	[26]
	$HO_2+OH=H_2O+O_2$	9.27E+15	0	17500	[26]
18a	$HO_2+HO_2=H_2O_2+O_2$	1.03E+14	0	11040	[26]
	$HO_2+HO_2=H_2O_2+O_2$	1.94E+11	0	-1409	
18b	$HO_2+HO_2+M=H_2O_2+O_2+M$	6.84E+14	0	-1950	[26]
19	$H_2O_2+H=HO_2+H_2$	1.70E+12	0	3755	[26]
20	$H_2O_2+H=H_2O+OH$	1.00E+13	0	3575	[26]
21	$H_2O_2+O=HO_2+OH$	9.55E+06	2	3970	[26]
22	$H_2O_2+OH=HO_2+H_2O$	2.00E+12	0	427	[26]
23	$O+O+M=O_2+M^a$	1.00E+17	-1.0	0	
	Enhanced third-body efficiencies (relative to Ar): N ₂ = 2, O = 28.8, O ₂ = 8, NO = 2, N = 2, N ₂ O = 4.38				[46]
24	$N_2+M=N+N+M^a$	1.00E+28	-3.33	225000	[46]
	Enhanced third-body efficiencies (relative to Ar): N ₂ = 2.96, O ₂ = 2.96, NO = 2.96, N = 6.6, O = 6.6				
		1.8E+14	0	76300	[46]
25	$N_2+O=NO+N$	5.85E+09	1.01	6200	[46]
26	$N+O_2=NO+O$	7.71E+19	-1.31	150000	[46]
27	$NO+M=N+O+M^a$				
	Enhanced third-body efficiencies (relative to Ar): NO = 3, N ₂ = 1.5				
		3.0E+11	0	65000	[46]
28	$NO+NO=N_2+O_2$	9.9E+10	0	57900	[46]
29	$N_2O(+M)=N_2+O(+M)^{a,b}$	6.0E+14	0	57440	[46]
	Low pressure limit: F _{cent} = 1.167-1.25e-04 T Enhanced third-body efficiencies (relative to Ar): O ₂ = 1.4, N ₂ = 1.7, N ₂ O = 3.5, NO = 3				
		3.69E+12	0	15940	[46]
30	$N_2O+O=N_2+O_2$	9.15E+13	0	27680	[46]
31	$N_2O+O=NO+NO$	2.50E+12	0	20000	[46]
32	$N_2O+N=N_2+NO$	2.75E+14	0	50000	[46]
33	$N_2O+NO=N_2+NO_2$	2.9E+14	-0.4	0	[46]
34	$NO+O(+M)=NO_2(+M)^{a,b}$	2.3E+20	-1.6	0	[46]
	Low pressure limit: F _{cent} = 0.8 Enhanced third-body efficiencies (relative to Ar): N ₂ = 1.46, O ₂ =1.3, NO = 2.8, NO ₂ = 10, N ₂ O = 7				
		3.3E+12	0	-374	[46]
35	$NO_2+O=NO+O_2$	8.0E+11	0	-437	[46]
36	$NO_2+N=NO+NO$	1.0E+12	0	-437	[46]
37	$NO_2+N=N_2O+O$	1.0E+12	0	60000	[46]
38	$NO_2+NO=N_2O+O_2$				

39	$\text{NO}_2+\text{NO}_2=\text{NO}+\text{NO}+\text{O}_2$	3.95E+12	0	27590	[46]
40	$\text{NO}_2+\text{NO}_2=\text{NO}_3+\text{NO}$	1.13E+04	2.58	22720	[46]
41	$\text{NO}_2+\text{O}(+\text{M})=\text{NO}_3(+\text{M})^{\text{a,b}}$	3.5E+12	0.24	0	[46]
	Low pressure limit:	2.4E+20	-1.5	0	[46]
	$F_{\text{cent}} = 0.71 * \exp(-T/1700)$				
	Enhanced third-body efficiencies (relative to N_2):				
	$\text{Ar}=1.2$				
42	$\text{NO}_3=\text{NO}+\text{O}_2$	2.5E+06	0	12120	[46]
43	$\text{NO}_3+\text{O}=\text{NO}_2+\text{O}_2$	1.0E+13	0	0	[46]
44	$\text{NO}_3+\text{NO}_2=\text{NO}+\text{NO}_2+\text{O}_2$	1.51E+10	0	2440	[46]
45	$\text{NO}_3+\text{NO}_3=\text{NO}_2+\text{NO}_2+\text{O}_2$	5.1E+11	0	4870	[46]
46	$\text{N}_2\text{O}_4(+\text{M})=\text{NO}_2+\text{NO}_2(+\text{M})^{\text{a,b}}$	1.15E+16	0	12840	[46]
	Low pressure limit:	2.0E+28	-3.8	12720	[46]
	$F_{\text{cent}} = 0.4$				
	Enhanced third-body efficiencies (relative to N_2):				
	$\text{Ar} = 0.8, \text{N}_2\text{O}_4 = 2, \text{NO}_2 = 2$				
47	$\text{N}_2\text{O}_4+\text{O}=\text{N}_2\text{O}_3+\text{O}_2$	1.21E+12	0	0	[46]
48	$\text{NO}_2+\text{NO}(+\text{M})=\text{N}_2\text{O}_3(+\text{M})^{\text{a,b}}$	1.6E+09	1.4	0	[46]
	Low pressure limit:	1.0E+33	-7.7	0	[46]
	$F_{\text{cent}} = 0.6$				
	Enhanced third-body efficiencies (relative to Ar):				
	$\text{N}_2 = 1.36$		[43]		
49	$\text{N}_2\text{O}_3+\text{O}=\text{NO}_2+\text{NO}_2$	2.71E+11	0	0	[46]
50	$\text{NO}_2+\text{N}=\text{N}_2+\text{O}_2$	2.4E+11	0	-437	[46]
51	$\text{NO}+\text{NO}+\text{NO}=\text{N}_2\text{O}+\text{NO}_2$	1.07E+10	0	26800	[46]
52	$\text{NH}+\text{M}=\text{N}+\text{H}+\text{M}$	2.65E+14	0	75500	[30]
53	$\text{NH}+\text{H}=\text{N}+\text{H}_2$	3.20E+13	0	325	[30]
54	$\text{NH}+\text{N}=\text{N}_2+\text{H}$	9.00E+11	0.5	0	[30]
55	$\text{NH}+\text{NH}=\text{NNH}+\text{H}$	5.10E+13	0	0	[30]
56	$\text{NH}+\text{NH}=\text{NH}_2+\text{N}$	5.95E+02	2.89	-2030	[30]
57	$\text{NH}+\text{NH}=\text{N}_2+\text{H}_2$	1.00E+08	1	0	[30]
58	$\text{NH}_2+\text{M}=\text{NH}+\text{H}+\text{M}$	3.16E+23	-2	91400	[30]
59	$\text{NH}+\text{H}_2=\text{NH}_2+\text{H}$	1.00E+14	0	20070	[30]
60	$\text{NH}_2+\text{N}=\text{N}_2+\text{H}+\text{H}$	6.90E+13	0	0	[30]
61	$\text{NH}_2+\text{NH}=\text{N}_2\text{H}_2+\text{H}$	1.50E+15	-0.5	0	[30]
62	$\text{NH}_2+\text{NH}=\text{NH}_3+\text{N}$	1.00E+13	0	2000	[30]
63	$\text{NH}_3+\text{NH}=\text{NH}_2+\text{NH}_2$	3.16E+14	0	26770	[30]
64	$\text{NH}_2+\text{NH}_2=\text{N}_2\text{H}_2+\text{H}_2$	1.00E+13	0	1500	[30]
65	$\text{N}_2\text{H}_3+\text{H}=\text{NH}_2+\text{NH}_2$	5.00E+13	0	2000	[30]
66	$\text{NH}_3+\text{M}=\text{NH}_2+\text{H}+\text{M}$	2.20E+16	0	93470	[30]

67	$\text{NH}_3+\text{M}=\text{NH}+\text{H}_2+\text{M}$	6.30E+14	0	93390	[30]
68	$\text{NH}_3+\text{H}=\text{NH}_2+\text{H}_2$	5.42E+05	2.4	9920	[30]
69	$\text{NH}_3+\text{NH}_2=\text{N}_2\text{H}_3+\text{H}_2$	1.00E+11	0.5	21600	[30]
70	$\text{NNH}=\text{N}_2+\text{H}$	3.00E+08	0	0	[30]
71	$\text{NNH}+\text{M}=\text{N}_2+\text{H}+\text{M}$	1.00E+13	0.5	3060	[30]
72	$\text{NNH}+\text{H}=\text{N}_2+\text{H}_2$	1.00E+14	0	0	[30]
73	$\text{NNH}+\text{N}=\text{NH}+\text{N}_2$	3.00E+13	0	2000	[30]
74	$\text{NNH}+\text{NH}=\text{N}_2+\text{NH}_2$	2.00E+11	0.5	2000	[30]
75	$\text{NNH}+\text{NH}_2=\text{N}_2+\text{NH}_3$	1.00E+13	0	0	[30]
76	$\text{NNH}+\text{NNH}=\text{N}_2\text{H}_2+\text{N}_2$	1.00E+13	0	4000	[30]
77	$\text{N}_2\text{H}_2+\text{M}=\text{NNH}+\text{H}+\text{M}$ Enhanced third-body efficiency $\text{H}_2\text{O}=15, \text{O}_2=2, \text{N}_2=2$	5.00E+16	0	50000	[30]
78	$\text{N}_2\text{H}_2+\text{M}=\text{NH}+\text{NH}+\text{M}$ Enhanced third-body efficiency $\text{H}_2\text{O}=15, \text{O}_2=2, \text{N}_2=2$	3.16E+16	0	99400	[30]
79	$\text{N}_2\text{H}_2+\text{H}=\text{NNH}+\text{H}_2$	8.50E+04	2.63	-230	[30]
80	$\text{N}_2\text{H}_2+\text{N}=\text{NNH}+\text{NH}$	1.00E+06	2	0	[30]
81	$\text{N}_2\text{H}_2+\text{NH}=\text{NNH}+\text{NH}_2$	1.00E+13	0	6000	[30]
82	$\text{N}_2\text{H}_2+\text{NH}_2=\text{NH}_3+\text{NNH}$	8.80E-02	4.05	-1610	[30]
83	$\text{N}_2\text{H}_3+\text{NH}=\text{N}_2\text{H}_2+\text{NH}_2$	2.00E+13	0	0	[30]
84	$\text{N}_2\text{H}_3+\text{NNH}=\text{N}_2\text{H}_2+\text{N}_2\text{H}_2$	1.00E+13	0	4000	[30]
85	$\text{N}_2\text{H}_3+\text{M}=\text{NH}_2+\text{NH}+\text{M}$	5.00E+16	0	60000	[30]
86	$\text{N}_2\text{H}_3+\text{M}=\text{N}_2\text{H}_2+\text{H}+\text{M}$	1.00E+16	0	37000	[30]
87	$\text{N}_2\text{H}_3+\text{H}=\text{N}_2\text{H}_2+\text{H}_2$	1.00E+13	0	0	[30]
88	$\text{N}_2\text{H}_3+\text{H}=\text{NH}+\text{NH}_3$	1.00E+11	0	0	[30]
89	$\text{N}_2\text{H}_3+\text{N}=\text{N}_2\text{H}_2+\text{NH}$	1.00E+06	2	0	[30]
90	$\text{N}_2\text{H}_3+\text{NH}_2=\text{NH}_3+\text{N}_2\text{H}_2$	1.00E+11	0.5	0	[30]
91	$\text{N}_2\text{H}_3+\text{N}_2\text{H}_2=\text{N}_2\text{H}_4+\text{NNH}$	1.00E+13	0	6000	[30]
92	$\text{N}_2\text{H}_3+\text{N}_2\text{H}_3=\text{NH}_3+\text{NH}_3+\text{N}_2$	3.00E+12	0	0	[30]
93	$\text{N}_2\text{H}_3+\text{N}_2\text{H}_3=\text{N}_2\text{H}_4+\text{N}_2\text{H}_2$	1.20E+13	0	0	[30]
94	$\text{N}_2\text{H}_4(+\text{M})=\text{NH}_2+\text{NH}_2(+\text{M})$ Low pressure: Enhanced third-body efficiency $\text{N}_2=2.4, \text{NH}_3=3.0, \text{N}_2\text{H}_4=4.0$	5.00E+14 1.50E+15	0 0	60000 39000	[30]
95	$\text{N}_2\text{H}_4+\text{M}=\text{N}_2\text{H}_3+\text{H}+\text{M}$	1.00E+15	0	63600	[30]
96	$\text{N}_2\text{H}_4+\text{H}=\text{N}_2\text{H}_3+\text{H}_2$	7.00E+12	0	2500	[30]
97	$\text{N}_2\text{H}_4+\text{H}=\text{NH}_2+\text{NH}_3$	2.40E+09	0	3100	[30]
98	$\text{N}_2\text{H}_4+\text{N}=\text{N}_2\text{H}_3+\text{NH}$	1.00E+10	1	2000	[30]
99	$\text{N}_2\text{H}_4+\text{NH}=\text{NH}_2+\text{N}_2\text{H}_3$	1.00E+09	1.5	2000	[30]
100	$\text{N}_2\text{H}_4+\text{NH}_2=\text{N}_2\text{H}_3+\text{NH}_3$	1.80E+06	1.71	-1380	[30]
101	$\text{N}+\text{OH}=\text{NO}+\text{H}$	2.80E+13	0	0	[30]
102	$\text{N}_2\text{O}+\text{H}=\text{N}_2+\text{OH}$	2.20E+14	0	16750	[30]
103	$\text{N}_2\text{O}+\text{H}=\text{NH}+\text{NO}$	6.70E+22	-2.16	37155	[30]
104	$\text{N}_2\text{O}+\text{H}=\text{NNH}+\text{O}$	5.50E+18	-1.06	47290	[30]
105	$\text{N}_2\text{O}+\text{H}=\text{HNNO}$	8.00E+24	-4.39	10530	[30]
106	$\text{N}_2\text{O}+\text{OH}=\text{N}_2+\text{HO}_2$	1.00E+14	0	30000	[30]
107	$\text{HNO}+\text{NO}=\text{N}_2\text{O}+\text{OH}$	8.50E+12	0	29580	[30]

108	$\text{HNO}+\text{NO}+\text{NO}=\text{HNNO}+\text{NO}_2$	1.60E+11	0	2090	[30]
109	$\text{NH}+\text{NO}+\text{M}=\text{HNNO}+\text{M}$	1.63E+23	-2.6	1820	[16]
110	$\text{HNNO}+\text{H}=\text{N}_2\text{O}+\text{H}_2$	2.00E+13	0	0	[16]
111	$\text{HNNO}+\text{H}=\text{NH}_2+\text{NO}$	1.00E+12	0	0	[16]
112	$\text{HNNO}+\text{O}=\text{N}_2\text{O}+\text{OH}$	2.00E+13	0	0	[16]
113	$\text{HNNO}+\text{OH}=\text{H}_2\text{O}+\text{N}_2\text{O}$	2.00E+13	0	0	[16]
114	$\text{HNNO}+\text{OH}=\text{HNOH}+\text{NO}$	1.00E+12	0	0	[16]
115	$\text{HNNO}+\text{NO}=\text{N}_2+\text{HONO}$	2.60E+11	0	1610	[16]
116	$\text{HNNO}+\text{NO}=\text{NNH}+\text{NO}_2$	3.20E+12	0	540	[16]
117	$\text{HNNO}+\text{NO}=\text{N}_2\text{O}+\text{HNO}$	1.00E+12	0	0	[16]
118	$\text{HNNO}+\text{NO}_2=\text{N}_2\text{O}+\text{HONO}$	1.00E+12	0	0	[16]
119	$\text{HNNO}+\text{NO}_2=\text{NNH}+\text{NO}_3$	1.00E+13	0	17000	[16]
120	$\text{NO}_2+\text{H}=\text{NO}+\text{OH}$	1.32E+14	0	362	[16]
121	$\text{NO}_2+\text{OH}=\text{HO}_2+\text{NO}$	1.81E+13	0	6676	[16]
122	$\text{NO}_2+\text{HO}_2=\text{HONO}+\text{O}_2$	4.64E+11	0	-479	[16]
123	$\text{NO}_2+\text{H}_2=\text{HONO}+\text{H}$	8.43E+03	2.635	32550	[1]
124	$\text{NO}_2+\text{NH}=\text{N}_2\text{O}+\text{OH}$	8.65E+10	0	-2270	[16]
125	$\text{NO}_2+\text{NH}=\text{NO}+\text{HNO}$	1.25E+11	0	-2270	[16]
126	$\text{NO}_3+\text{H}=\text{NO}_2+\text{OH}$	6.62E+13	0	0	[16]
127	$\text{NO}_3+\text{OH}=\text{NO}_2+\text{HO}_2$	1.21E+13	0	0	[16]
128	$\text{NO}_3+\text{HO}_2=\text{HNO}_3+\text{O}_2$	5.55E+11	0	0	[16]
129	$\text{NO}_3+\text{HO}_2=\text{NO}_2+\text{OH}+\text{O}_2$	1.51E+12	0	0	[16]
130	$\text{N}_2\text{O}_4+\text{H}_2\text{O}=\text{HONO}+\text{HNO}_3$	2.52E+14	0	11590	[16]
131	$\text{N}_2\text{O}_3+\text{H}_2\text{O}=\text{HONO}+\text{HONO}$	3.79E+13	0	8880	[16]
132	$\text{H}+\text{NO}(+\text{M})=\text{HNO}(+\text{M})$	1.52E+15	-0.41	0	[16]
133	$\text{HNO}+\text{H}=\text{NO}+\text{H}_2$	4.46E+11	0.72	655	[16]
134	$\text{HNO}+\text{OH}=\text{NO}+\text{H}_2\text{O}$	1.30E+07	1.88	-956	[16]
135	$\text{HNO}+\text{O}=\text{OH}+\text{NO}$	5.00E+11	0.5	2000	[16]
136	$\text{HNO}+\text{O}=\text{NO}_2+\text{H}$	5.00E+10	0	2000	[16]
137	$\text{HNO}+\text{O}_2=\text{NO}+\text{HO}_2$	2.20E+10	0	9140	[16]
138	$\text{HNO}+\text{N}=\text{NO}+\text{NH}$	1.00E+11	0.5	2000	[16]
139	$\text{HNO}+\text{N}=\text{H}+\text{N}_2\text{O}$	5.00E+10	0.5	3000	[16]
140	$\text{HNO}+\text{NH}=\text{NH}_2+\text{NO}$	5.00E+11	0.5	0	[16]
141	$\text{HNO}+\text{NH}_2=\text{NH}_3+\text{NO}$	2.31E+04	2.47	-2880	[41]
		1.55E+02	3.15	-3640	
142	$\text{HNO}+\text{HNO}=\text{N}_2\text{O}+\text{H}_2\text{O}$	3.63E-03	3.98	1190	[16]
143	$\text{HNO}+\text{HNO}=\text{HNOH}+\text{NO}$	2.00E+08	0	4170	[16]
144	$\text{HNO}+\text{NO}_2=\text{HONO}+\text{NO}$	6.02E+11	0	2000	[16]
145	$\text{NO}+\text{OH}(+\text{M})=\text{HONO}(+\text{M})$	2.00E+12	-0.05	-721	[16]
146	$\text{NO}_2+\text{H}+\text{M}=\text{HONO}+\text{M}$	1.40E+18	-1.5	900	[16]
147	$\text{HONO}+\text{H}=\text{HNO}+\text{OH}$	5.64E+10	0.86	4970	[16]
148	$\text{HONO}+\text{H}=\text{NO}+\text{H}_2\text{O}$	8.12E+06	1.89	3840	[16]
149	$\text{HONO}+\text{O}=\text{OH}+\text{NO}_2$	1.20E+13	0	5960	[16]
150	$\text{HONO}+\text{OH}=\text{H}_2\text{O}+\text{NO}_2$	1.69E+12	0	-517	[16]
151	$\text{HONO}+\text{NH}=\text{NH}_2+\text{NO}_2$	1.00E+13	0	0	[16]
152	$\text{HONO}+\text{HONO}=\text{H}_2\text{O}+\text{NO}_2+\text{NO}$	1.00E+13	0	8540	[16]

153	$\text{HONO} + \text{NH}_2 = \text{NO}_2 + \text{NH}_3$	1.02E+04	2.34	-3202	[42]
		4.84E+02	3.36	-4575	
154	$\text{NO}_2 + \text{OH} (+\text{M}) = \text{HNO}_3 (+\text{M})$	2.41E+13	0	0	[16]
155	$\text{NO} + \text{HO}_2 + \text{M} = \text{HNO}_3 + \text{M}$	1.50E+24	-3.5	2200	[16]
156	$\text{HNO}_3 + \text{H} = \text{H}_2 + \text{NO}_3$	5.56E+08	1.53	16400	[16]
157	$\text{HNO}_3 + \text{H} = \text{H}_2\text{O} + \text{NO}_2$	6.08E+01	3.29	6290	[16]
158	$\text{HNO}_3 + \text{H} = \text{OH} + \text{HONO}$	3.82E+05	2.3	6980	[16]
159	$\text{HNO}_3 + \text{OH} = \text{NO}_3 + \text{H}_2\text{O}$	1.03E+10	0	-1240	[16]
160	$\text{HNO}_3 + \text{NH}_2 = \text{NH}_3 + \text{NO}_3$	1.03E+21	-3.85	191	[43]
		3.08E+01	3.22	-139	
161	$\text{NH}_3 + \text{O} = \text{NH}_2 + \text{OH}$	1.10E+06	2.1	5210	[16]
162	$\text{NH}_3 + \text{OH} = \text{NH}_2 + \text{H}_2\text{O}$	5.00E+07	1.6	950	[16]
163	$\text{NH}_3 + \text{HO}_2 = \text{NH}_2 + \text{H}_2\text{O}_2$	3.00E+11	0	22000	[16]
164	$\text{NH}_2 + \text{HO}_2 = \text{NH}_3 + \text{O}_2$	1.65E+04	1.55	2027	[16]
165	$\text{NH}_2 + \text{O} = \text{H}_2 + \text{NO}$	5.00E+12	0	0	[16]
166	$\text{NH}_2 + \text{O} = \text{HNO} + \text{H}$	4.50E+13	0	0	[16]
167	$\text{NH}_2 + \text{O} = \text{NH} + \text{OH}$	7.00E+12	0	0	[16]
168	$\text{NH}_2 + \text{OH} = \text{NH} + \text{H}_2\text{O}$	9.00E+07	1.5	-460	[16]
169	$\text{NH}_2 + \text{OH} = \text{NH}_2\text{OH}$	1.79E+13	0.2	0	[16]
170	$\text{NH}_2 + \text{HO}_2 = \text{HNO} + \text{H}_2\text{O}$	5.68E+15	-1.12	707	[16]
171	$\text{NH}_2 + \text{HO}_2 = \text{H}_2\text{NO} + \text{OH}$	2.91E+17	-1.32	1248	[16]
172	$\text{NH}_2 + \text{O}_2 = \text{HNO} + \text{OH}$	1.00E+13	0	26290	[16]
173	$\text{NH}_2 + \text{O}_2 = \text{H}_2\text{NO} + \text{O}$	6.00E+13	0	29880	[16]
174	$\text{NH}_2 + \text{NO} = \text{NNH} + \text{OH}$	2.29E+10	0.425	-814	[16]
175	$\text{NH}_2 + \text{NO} = \text{N}_2 + \text{H}_2\text{O}$	2.77E+20	-2.65	1258	[16]
176	$\text{NH}_2 + \text{NO} = \text{H}_2 + \text{N}_2\text{O}$	1.00E+13	0	33700	[16]
177	$\text{NH}_2 + \text{NO}_2 = \text{N}_2\text{O} + \text{H}_2\text{O}$	1.62E+16	-1.44	270	[16]
178	$\text{NH}_2 + \text{NO}_2 = \text{H}_2\text{NO} + \text{NO}$	6.48E+16	-1.44	270	[16]
179	$\text{NH} + \text{O} = \text{NO} + \text{H}$	7.00E+13	0	0	[16]
180	$\text{NH} + \text{O} = \text{N} + \text{OH}$	7.00E+12	0	0	[16]
181	$\text{NH} + \text{OH} = \text{HNO} + \text{H}$	2.00E+13	0	0	[16]
182	$\text{NH} + \text{OH} = \text{N} + \text{H}_2\text{O}$	2.00E+09	1.2	0	[16]
183	$\text{NH} + \text{OH} = \text{NO} + \text{H}_2$	2.00E+13	0	0	[16]
184	$\text{NH} + \text{HO}_2 = \text{HNO} + \text{OH}$	1.00E+13	0	2000	[16]
185	$\text{NH} + \text{O}_2 = \text{HNO} + \text{O}$	4.00E+13	0	17880	[16]
186	$\text{NH} + \text{O}_2 = \text{NO} + \text{OH}$	4.50E+08	0.79	1190	[16]
187	$\text{NH} + \text{H}_2\text{O} = \text{NH}_2\text{OH}$	2.00E+13	0	13850	[16,47]
188	$\text{NH} + \text{N}_2\text{O} = \text{N}_2 + \text{HNO}$	2.00E+12	0	6000	[16]
189	$\text{NNH} + \text{O} = \text{NH} + \text{NO}$	1.00E+14	0	4000	[31]
190	$\text{NH} + \text{NO} = \text{N}_2 + \text{OH}$	6.10E+13	-0.5	120	[16]
191	$\text{N}_2\text{H}_4 + \text{O} = \text{N}_2\text{H}_2 + \text{H}_2\text{O}$	8.50E+13	0	1200	[16]
192	$\text{N}_2\text{H}_4 + \text{O} = \text{N}_2\text{H}_3 + \text{OH}$	2.50E+12	0	1200	[16]
193	$\text{N}_2\text{H}_4 + \text{OH} = \text{N}_2\text{H}_3 + \text{H}_2\text{O}$	3.00E+10	0.68	1290	[16]
194	$\text{N}_2\text{H}_4 + \text{OH} = \text{NH}_3 + \text{H}_2\text{NO}$	3.67E+13	0	0	[16]
195	$\text{N}_2\text{H}_4 + \text{HO}_2 = \text{N}_2\text{H}_3 + \text{H}_2\text{O}_2$	4.00E+13	0	2000	[16]
196	$\text{N}_2\text{H}_3 + \text{O} = \text{N}_2\text{H}_2 + \text{OH}$	2.00E+13	0	1000	[16]

197	$\text{N}_2\text{H}_3+\text{O}=\text{NNH}+\text{H}_2\text{O}$	3.16E+11	0.5	0	[16]
198	$\text{N}_2\text{H}_3+\text{O}=\text{NH}_2+\text{HNO}$	1.00E+13	0	0	[16]
199	$\text{N}_2\text{H}_3+\text{OH}=\text{N}_2\text{H}_2+\text{H}_2\text{O}$	3.00E+10	0.68	1290	[16]
200	$\text{N}_2\text{H}_3+\text{OH}=\text{NH}_3+\text{HNO}$	1.00E+12	0	15000	[16]
201	$\text{N}_2\text{H}_3+\text{O}_2=\text{N}_2\text{H}_2+\text{HO}_2$	3.00E+12	0	0	[16]
202	$\text{N}_2\text{H}_3+\text{HO}_2=\text{N}_2\text{H}_2+\text{H}_2\text{O}_2$	1.00E+13	0	2000	[16]
203	$\text{N}_2\text{H}_3+\text{HO}_2=\text{N}_2\text{H}_4+\text{O}_2$	8.00E+12	0	0	[16]
204	$\text{N}_2\text{H}_3+\text{NO}=\text{HNO}+\text{N}_2\text{H}_2$	1.00E+12	0	0	[16]
205	$\text{N}_2\text{H}_2+\text{O}=\text{NH}_2+\text{NO}$	1.00E+13	0	0	[16]
206	$\text{N}_2\text{H}_2+\text{O}=\text{NNH}+\text{OH}$	2.00E+13	0	1000	[16]
207	$\text{N}_2\text{H}_2+\text{OH}=\text{NNH}+\text{H}_2\text{O}$	5.92E+01	3.4	-1360	[16]
208	$\text{N}_2\text{H}_2+\text{HO}_2=\text{NNH}+\text{H}_2\text{O}_2$	1.00E+13	0	2000	[16]
209	$\text{N}_2\text{H}_2+\text{NO}=\text{N}_2\text{O}+\text{NH}_2$	3.00E+10	0	0	[16]
210	$\text{NNH}+\text{O}=\text{N}_2+\text{OH}$	1.70E+16	-1.23	500	[16]
211	$\text{NNH}+\text{OH}=\text{N}_2+\text{H}_2\text{O}$	2.40E+22	-2.88	2444	[16]
212	$\text{NNH}+\text{O}_2=\text{N}_2+\text{HO}_2$	1.20E+12	-0.34	150	[16]
213	$\text{NNH}+\text{O}_2=\text{N}_2\text{O}+\text{OH}$	2.90E+11	-0.34	150	[16]
214	$\text{NNH}+\text{HO}_2=\text{N}_2+\text{H}_2\text{O}_2$	1.00E+13	0	2000	[16]
215	$\text{NNH}+\text{NO}=\text{N}_2+\text{HNO}$	5.00E+13	0	0	[16]
216	$\text{NH}_2\text{OH}+\text{OH}=\text{HNOH}+\text{H}_2\text{O}$	2.50E+13	0	4250	[16]
217	$\text{H}_2\text{NO}+\text{M}=\text{H}_2+\text{NO}+\text{M}$ Enhanced third-body efficiency $\text{H}_2\text{O}=10.0$	7.83E+27	-4.29	60300	[16]
218	$\text{H}_2\text{NO}+\text{M}=\text{HNO}+\text{H}+\text{M}$ Enhanced third-body efficiency $\text{H}_2\text{O}=10.0$	2.80E+24	-2.83	64915	[16]
219	$\text{H}_2\text{NO}+\text{M}=\text{HNOH}+\text{M}$ Enhanced third-body efficiency $\text{H}_2\text{O}=10.0$	1.10E+29	-3.99	43980	[16]
220	$\text{H}_2\text{NO}+\text{H}=\text{HNO}+\text{H}_2$	3.00E+07	2	2000	[16]
221	$\text{H}_2\text{NO}+\text{H}=\text{NH}_2+\text{OH}$	5.00E+13	0	0	[16]
222	$\text{H}_2\text{NO}+\text{O}=\text{HNO}+\text{OH}$	3.00E+07	2	2000	[16]
223	$\text{H}_2\text{NO}+\text{OH}=\text{HNO}+\text{H}_2\text{O}$	2.00E+07	2	1000	[16]
224	$\text{H}_2\text{NO}+\text{HO}_2=\text{HNO}+\text{H}_2\text{O}_2$	2.90E+04	2.69	-1600	[16]
225	$\text{H}_2\text{NO}+\text{NH}_2=\text{HNO}+\text{NH}_3$	3.00E+12	0	1000	[16]
226	$\text{H}_2\text{NO}+\text{O}_2=\text{HNO}+\text{HO}_2$	3.00E+12	0	25000	[16]
227	$\text{H}_2\text{NO}+\text{NO}=\text{HNO}+\text{HNO}$	2.00E+07	2	13000	[16]
228	$\text{H}_2\text{NO}+\text{NO}_2=\text{HONO}+\text{HNO}$	6.00E+11	0	2000	[16]
229	$\text{HNOH}+\text{M}=\text{HNO}+\text{H}+\text{M}$ Enhanced third-body efficiency $\text{H}_2\text{O}=10.0$	2.00E+24	-2.84	58935	[16]
230	$\text{HNOH}+\text{H}=\text{HNO}+\text{H}_2$	4.80E+08	1.5	380	[16]
231	$\text{HNOH}+\text{H}=\text{NH}_2+\text{OH}$	4.00E+13	0	0	[16]
231	$\text{HNOH}+\text{O}=\text{HNO}+\text{OH}$	7.00E+13	0	0	[16]
		3.30E+08	1.5	-360	
232	$\text{HNOH}+\text{OH}=\text{HNO}+\text{H}_2\text{O}$	2.40E+06	2	-1190	[16]
233	$\text{HNOH}+\text{HO}_2=\text{HNO}+\text{H}_2\text{O}_2$	2.90E+04	2.69	-1600	[16]
234	$\text{HNOH}+\text{NH}_2=\text{HNO}+\text{NH}_3$	1.80E+06	1.94	-1150	[16]

235	$\text{HNOH} + \text{NO}_2 = \text{HONO} + \text{HNO}$	6.00E+11	0	2000	[16]
236	$\text{HNOH} + \text{O}_2 = \text{HNO} + \text{HO}_2$	3.00E+12	0	25000	[16]
237	$\text{HNOH} + \text{HNO} = \text{NH}_2\text{OH} + \text{NO}$	1.00E+12	0	3000	[16]

Modeling Details

The detailed reaction mechanism used in this study is listed in Table 1. All reactions are reversible; in the modeling, the reverse rate constants are calculated from the forward rate constants and thermodynamic data by the Chemkin chemical interpreter code [63] and the one dimensional laminar code CHEM1D developed at Eindhoven University of Technology [64]. Experiments in static reactors were modelled as a constant volume adiabatic process or isothermal process for characteristic times longer than 10 seconds. Shock-tube measurements were modelled as constant pressure or constant volume adiabatic processes using the SENKIN code and flames of nitrous oxide were calculated using the Premix code from the Chemkin Collection. Thermodynamic data used are all from the latest database of Burcat and Ruscic [65]. The sources of the rate constants are also shortly outlined. Also temperature range over which the rate constants were determined are presented. All rate coefficients in the present work are given in $\text{cm}^3 \cdot \text{mole}^{-1} \cdot \text{s}^{-1}$ units, while activation energies are in cal/mole .

The in-house CHEM1D 1-D [64] laminar code was used for modeling the combustion process in determining the flame speed. CHEM1D solves a set of equations describing the conservation of mass, momentum, energy and chemical components for chemically reacting flows. It uses an exponential finite volume discretization in space and the non linear differential equations are solved with a fully implicit, modified Newton method. An adaptive gridding procedure is also implemented to increase accuracy in the flame front by placing almost 80% of the gridpoints in the area with the largest gradients. The input to this code are the conditions (pressure, temperature, mixture composition), thermodynamic and transport data and the chemical reaction mechanism.

Simulations were performed for a number of conditions in examining their predictability by comparison with recent experimental data and other kinetic mechanisms. Experimental data at higher pressure with lean combustion was available for H_2 combustion with O_2 -He as oxidizer. He suppresses the thermo-diffusive instabilities at higher pressure. Although replacing N_2 in air with He does change the flame temperature and speed but not the fundamental chemistry.

Results and Discussion

The laminar burning velocity defines the rate with which the unburnt mixture is consumed in the propagating laminar flame. This parameter is considered one of the most important entities in assessing many phenomena like ignition, flame quenching, flashback stabilization etc. in burners and combustors. Along with its importance in designing combustors, this parameter also holds its importance in validating chemical kinetic mechanisms. For instance, H_2 /air mixture has burning velocity much higher than CH_4 /air. If the chemistry of H_2 /air at temperatures and pressures related to combustion conditions is understood and validated by comparing the simulation (using this chemistry) with experimentally found burning velocity, it in turn helps in simulating larger processes like turbulent flames etc.

Due to its attractiveness in power and automobile sector H_2 /air combustion studies have been done extensively in the past two decades. Fig 1 describes a simple variation of the burning velocity of H_2 /air mixture and various equivalence ratios (especially lean). One of the objectives of the present study is to analyze various reaction mechanisms that work well at lean and high pressure conditions. Grimech3.0 [2] is being used in various industrial applications for simulations as it covers many hydrocarbon combustion reactions. In the same line, H_2 combustion mechanism must not be utilized from GRImech3.0. The mechanism remains stable at atmospheric conditions with slight deviation for $\phi > 0.8$. Other available mechanisms[1,9] and present one roughly behave in the same order at least for $\phi < 0.8$. Measurement data from Tse et al.[10] have been utilized to validate the mechanisms at $P=1\text{atm}$ and $T=298\text{K}$. Other experimental data were also available from Aung et al. [6] and Dowdy et al. [66].

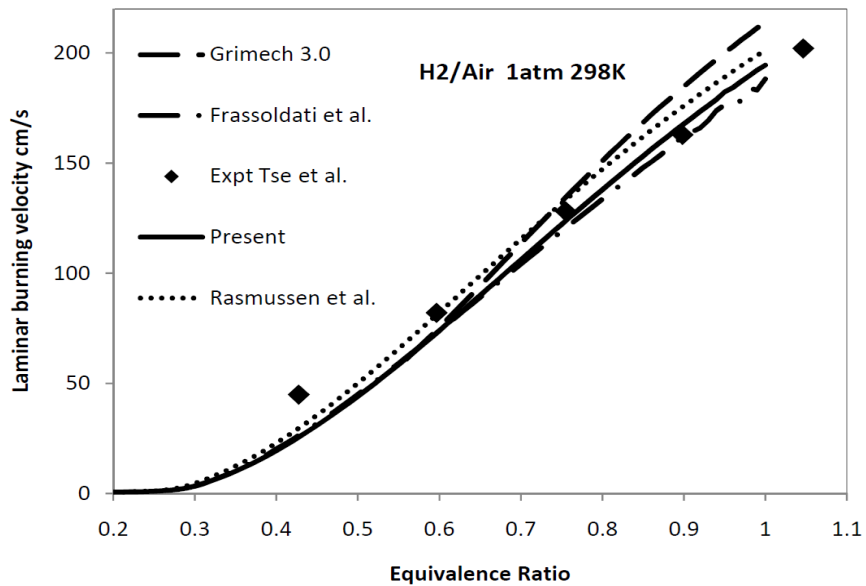


Fig 1: Variation of Laminar burning velocity of H_2 /air mixture at 1 atm and 298K with equivalence ratio.

From the literature, researchers have recently recommended the mechanism by Li et al.[19]. Studies by Skottene and Rian [20] and Strohle and Myhrvold [22] suggests that the hydrogen subset of Li mechanism and the NO_x subset of Glarborg produces good results at high pressures. To understand the reliability of the mechanism comparisons were done at high pressures. Fig 2-4 depict burning velocity variation with respect to equivalence ratio at pressures 10, 15 and 20 atm ($T=298\text{K}$) for $H_2/O_2/He$ system. O_2 in the oxidizer was 8% in this study. Experimental results of Tse et al [10] have been utilized for comparison. Similar comparison was made for 15 and 20 atm also.

These high pressure comparisons give certain indications. Firstly, the Li mechanism starts to drift from the expected curve with a difference of almost 5-10cm/s as the pressure increases. Secondly, the behaviour of GRImech3.0 results clearly show its unreliability in predicting burning velocities at higher pressure(even at 10 atm). Thirdly, the difference between the present and other models[1,9] is small. The mechanism by Frassoldati et al. [9] shows a small difference at $0.65 < \phi < 0.85$. At equivalence ratio < 0.65 , curves almost merge showing very small velocities.

Pressure dependences of the H₂/O₂/He combustion chemistry at lean condition of $\phi=0.85$ and T=298K are summarized in Fig 5. Grimech3.0 shows an offset behaviour even at 1atm. This depicts that this mechanism not only fails to simulate high pressure combustion but also lean mixtures at atmospheric pressure. Li mechanism performs satisfactorily when others perform reasonably well especially Rasmussen et al.[1] and the present mechanism.

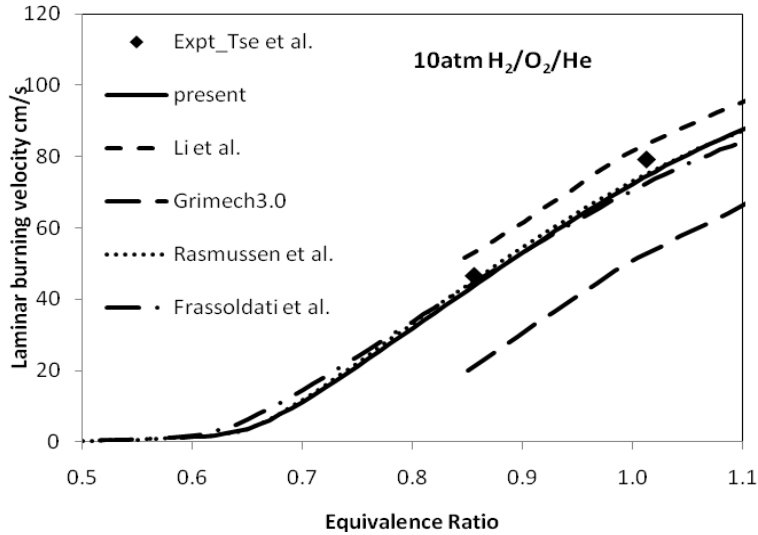


Fig 2: Comparison of simulation results of various mechanisms with experimental data for H₂/O₂/He mixtures at 10atm and 298K. (O₂/O₂+He=0.08)

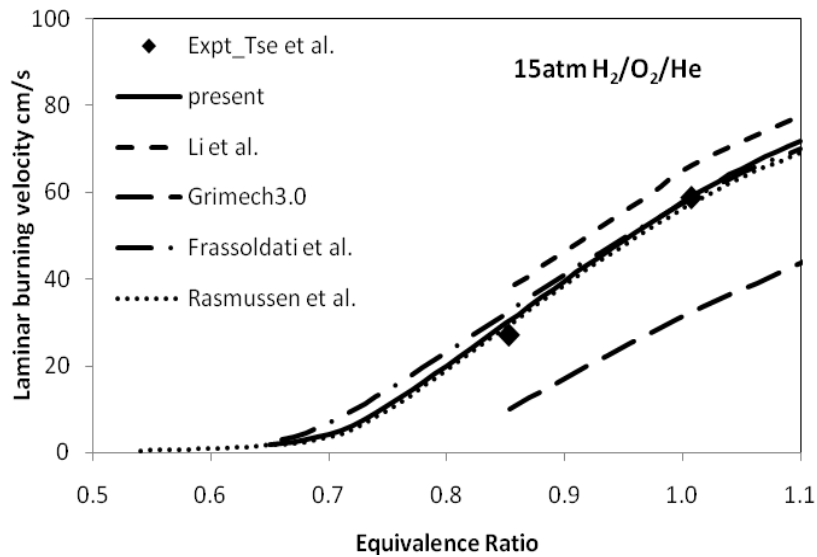


Fig 3: Comparison of simulation results of various mechanisms with experimental data for H₂/O₂/He mixtures at 15 atm and 298K. (O₂/O₂+He=0.08)

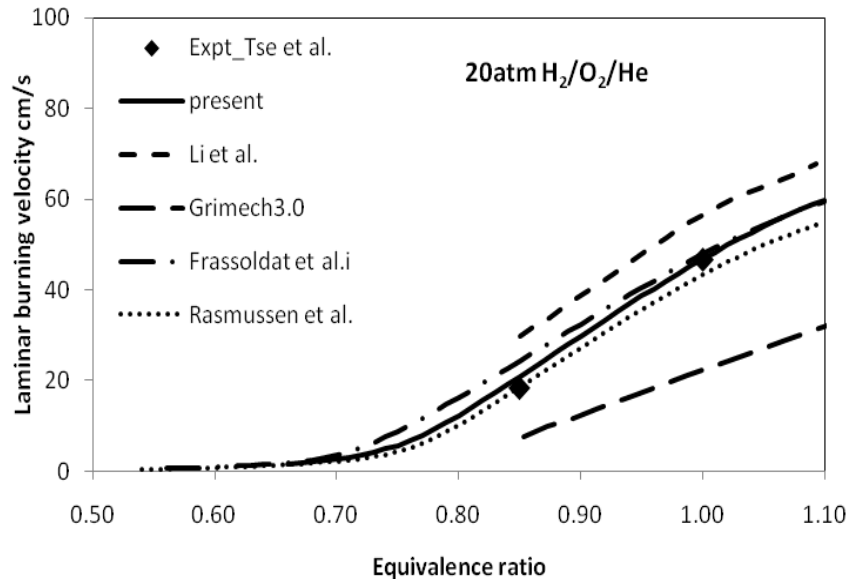


Fig 4: Comparison of simulation results of various mechanisms with experimental data for H₂/O₂/He mixtures at 20atm and 298K. (O₂/O₂+He=0.08)

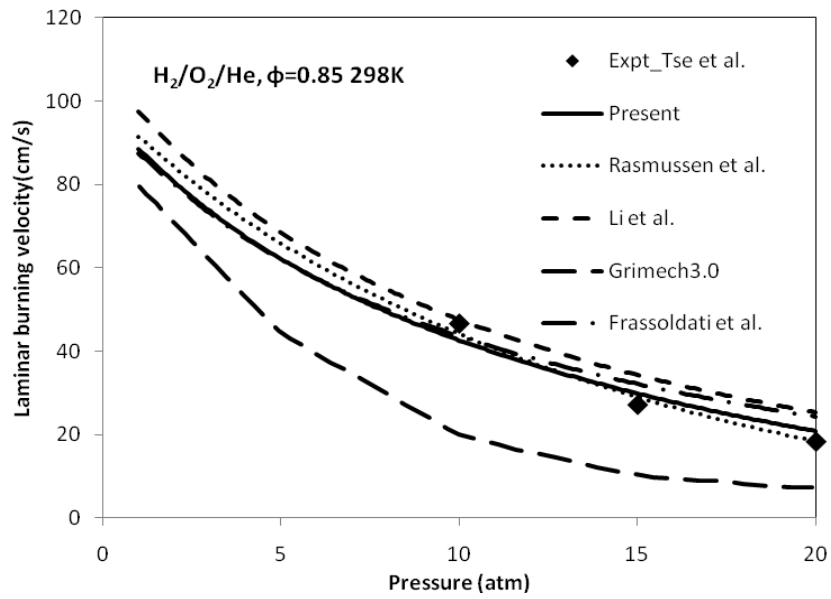


Fig 5: Comparison of simulation results of various mechanisms with experimental data for H₂/O₂/He mixtures at $\phi=0.85$ and 298K. (O₂/O₂+He=0.08)

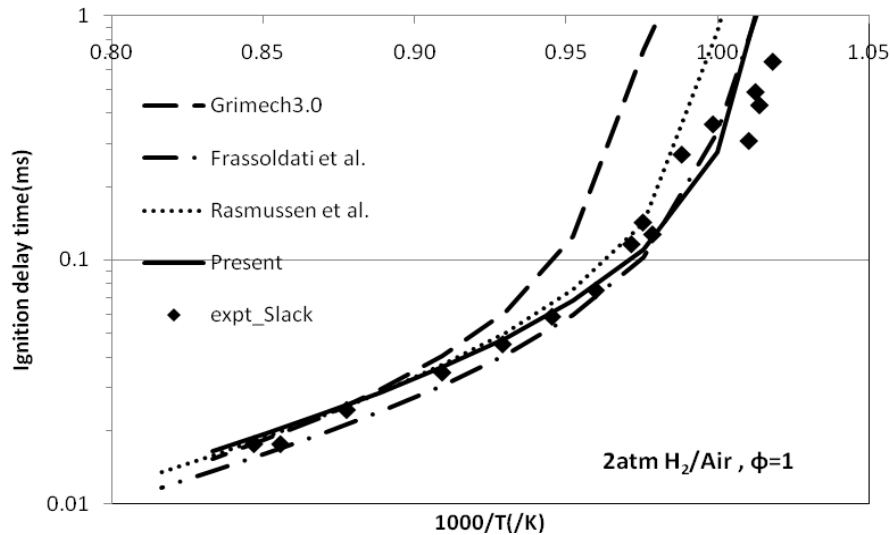
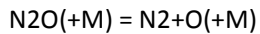


Fig 6: Comparison of simulation results of various mechanisms with experimental data for stoichiometric H₂/air mixtures at 2 atm.

Ignition delay is another parameter often used for validating reaction mechanism. Coupling of a reliable kinetic mechanism with a numerical flow solver accurately models reacting flow problems. Considerable amount of work has been done in analyzing differences in experimental data and predictions using kinetic models. Experimental data are drawn from shock tube, flow reactor and rapid compression experiments. These and many such studies have revealed disagreement between experimental data and model predictions. These experimentations have implied that there exists a lot of scope in improvement of rate constants when compared to flame speed and ignition delay data obtained.

Fig. 6 shows a comparison of model predicted (lines) ignition delay times (shown on a logarithmic scale) with experimental data available (points). The ignition delay time in the present study has been defined as the time when there is a temperature rise of 50 K after the ignition. There are a number of definitions out of which rise in OH concentration to a certain value defined for a particular mixture condition or a rapid increase in the pressure are the most popular in recent literature. The figure describes a H₂/air stoichiometric mixture ignited at 2 atm. For a temperature range from 1000K and higher the model predictions match more or less with the experiments [67]. The experimental data has been extracted from shock tube experiments of Slack [67]. In the case of determining ignition delay time also GRI mech 3.0 shows unsatisfactory predictions for lower temperatures. This is not the case with other mechanisms that more or less follow the trend.

Ignition delays in mixture of 20% of N₂O with Ar were measured in reflected shock waves by Borisov and Skachkov [68] for pressures 2.5-3.5 atm and 10-14 atm. Shock tube data were modelled at mean pressures of 3 and 12 atm, since the authors of [68] did not specify the pressure of individual experimental runs. Ignition delays were determined as times when rate of N₂O consumption reached its maximum value. Experimental data in comparison with the results of modelling are shown in Fig 7. At the conditions of these experiments the ignition delays are governed by the rate constant of decomposition reaction



(29)

Two rate constants have been tested: recommended by Baulch et al.[49] and derived recently by Javoy et al. [69]. As expected, modelling with k of Javoy et al. [69] (the highest rate constant of the two) gives shorter ignition times than modelling with k of Baulch et al.[49] Fig 7 shows that modelling with k of Javoy et al.[69] provides a good agreement with the experimental data for a pressure of 12 atm. It cannot describe equally well the experimental data for 3 atm, but the agreement is still satisfactory. The mechanism with k of Baulch et al. performs a little better at 3 atm, but in general the use of k of Javoy et al. provides better agreement with this set of the experimental data.

Sulzmann et al. [70] measured specific rate constants of nitrous oxide decomposition in mixtures of 2% N_2O with Ar using reflected shock-waves. The experiments were conducted over a temperature range of 1720-2554 K at pressures of 1.7-4.55 atm. The specific rate constants were determined using initial rates of N_2O disappearance using the equation: $d[\text{N}_2\text{O}]/dt = -k_{\text{eff}}[\text{M}][\text{N}_2\text{O}]$. The experimental results are compared with results of calculations in Fig. 8. As expected, modelling with k of Javoy et al. [69] gives higher specific rate constants, which are closer to the experimental data [70] than those obtained using k of Baulch et al.[49]. The experimental data fall into two groups: 1) those obtained at $T \leq 2215$ K and 2) at $T > 2215$ K. At temperatures up to 2215 K the agreement between the experimental data and the results of modelling with k of Javoy et al.[69] is very good. However, at higher temperatures the agreement is worse – results of the modelling are lower than the experimental data by ~60%.

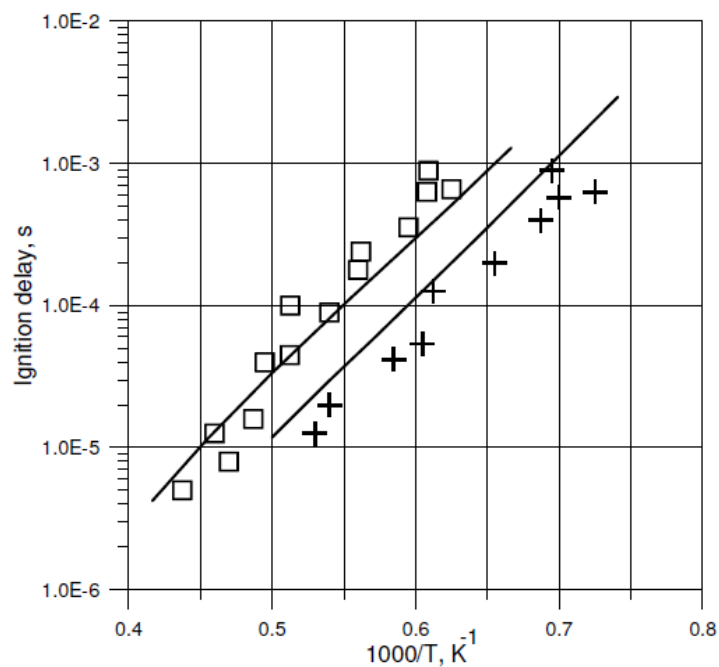


Fig 7: Mixture of 20% N_2O with Ar. Squares -2.2-3.5atm[68], crosses-10-14atm[68], Lines-modeling[46]

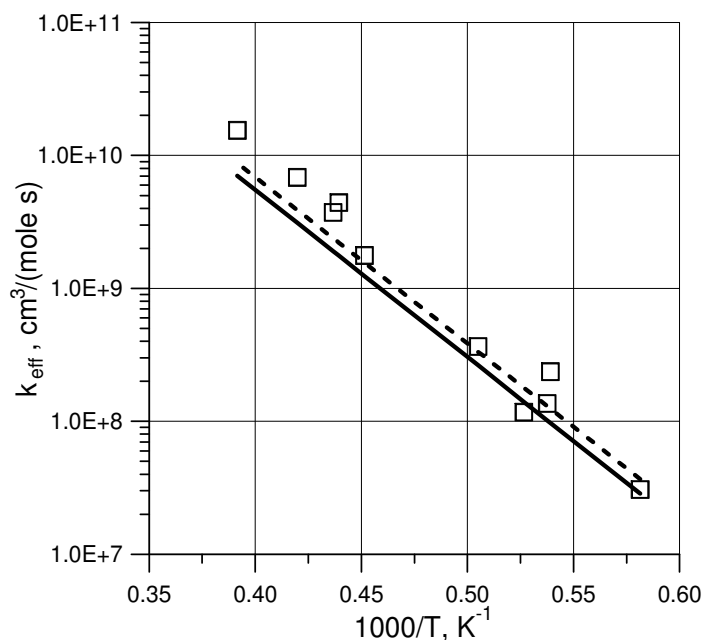


Fig. 8. Specific rate constant of N_2O decomposition in N_2O -Ar mixtures containing 2% N_2O , $P_0=1.7$ - 4.55 atm. Squares – Sulzmann et al. [70], solid line – modelling with k recommended by Baulch et al. [49], dashed line – modelling with k recommended by Javoy et al.[69].

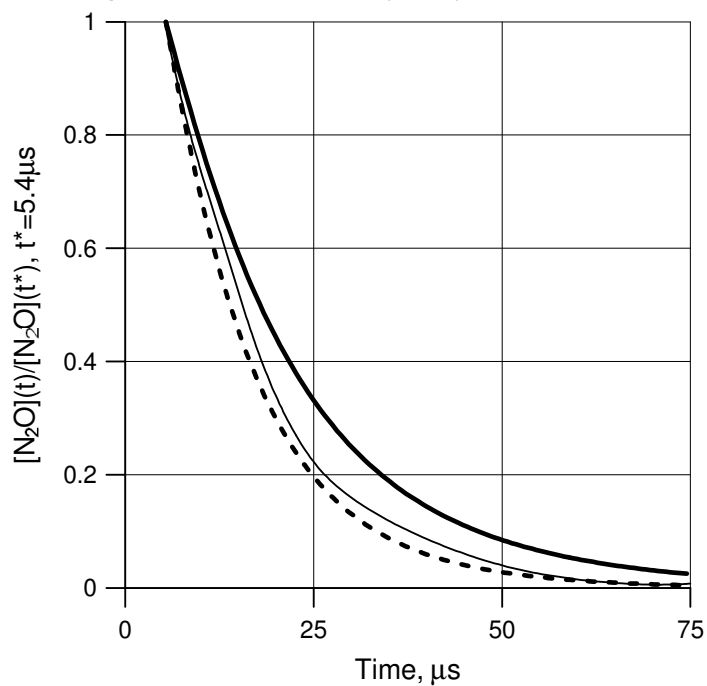


Fig. 9. N_2O decay in mixture of 2032 ppm N_2O with Ar, $T_0=2047$ K and $P_0=43.1$ atm. Solid thin line – experimental data of Röhrig et al. [58], solid thick line – modelling with k recommended by Baulch et al.[49], dashed line – modelling with k recommended Javoy et al.[69].

Fig 9 shows nitrous oxide concentration profile measured behind a reflected shock wave using IR emission ($4.5 \mu\text{m}$) [58]. The profile is normalized to a value of the signal at a time $t^*=5.4 \mu\text{s}$. These experimental data (measured at a pressure of 43.1 atm) are the highest-pressure data that were used for validation of the mechanism. At this high pressure the use of k of Baulch et al.[49] also leads to the noticeable underestimation of the rate of N_2O decay, as in the case of low-pressure data ($P_0 \approx 2 \text{ atm}$) of [71]. The modelling with k of Javoy et al.[69] provides much better agreement with the experimental data, even though it slightly overestimates the rate of N_2O decay.

A comparison of NO formation in $\text{H}_2/\text{O}_2/\text{N}_2$ flames is depicted in Fig 10 and 11. Homer and Sutton[72] performed experiments at atmospheric pressure to obtain nitric oxide [NO] concentration in premixed hydrogen-oxygen-nitrogen flames (reactant composition by volume being: $2\text{H}_2+1.4\text{O}_2+7.6\text{N}_2$, $2\text{H}_2+1.4\text{O}_2+6.1\text{N}_2$, $2\text{H}_2+1.4\text{O}_2+5.3\text{N}_2$ and $2\text{H}_2+1.4\text{O}_2+4.6\text{N}_2$). The change in N_2 percentage significantly changed the flame temperature. These results have been used for comparison with mechanisms from literature[1,2,9] and the present mechanism. GRI mech 3.0[2] shows unsatisfactory results in all the cases. Prediction by mechanism of Rasmussen et al.[1] seems to be better than all others. Konnov[38] argued that the relative importance of NNH route also varies with temperature (like thermal NO) and is dominant below 2000K. Hence, downstream (after 2cm) drops as only thermal NO_x mechanism remains.

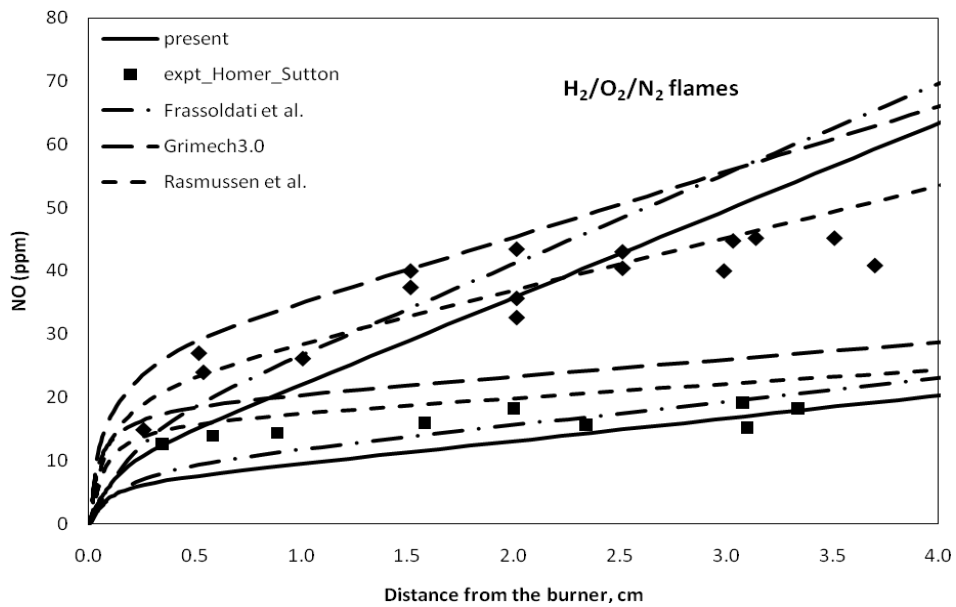


Fig 10: Comparison of profiles of NO along flames of $\text{H}_2/\text{O}_2/\text{N}_2$ mixtures at 1 atm. Lines: simulation results of various mechanisms, Symbols: experimental data[72]. Square: $2\text{H}_2+1.4\text{O}_2+5.3\text{N}_2$, Diamond: $2\text{H}_2+1.4\text{O}_2+4.6\text{N}_2$.

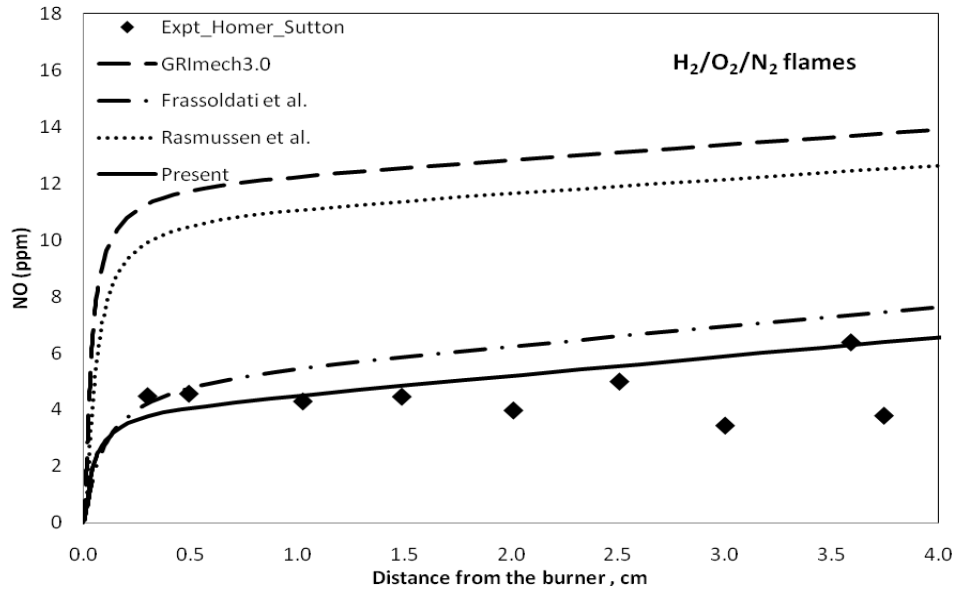


Fig 11: Comparison of profiles of NO along flames of H₂/O₂/N₂ mixture(2H₂+1.4O₂+6.1N₂) at 1 atm. Lines: simulation results of various mechanisms, Symbols: experimental data[72]

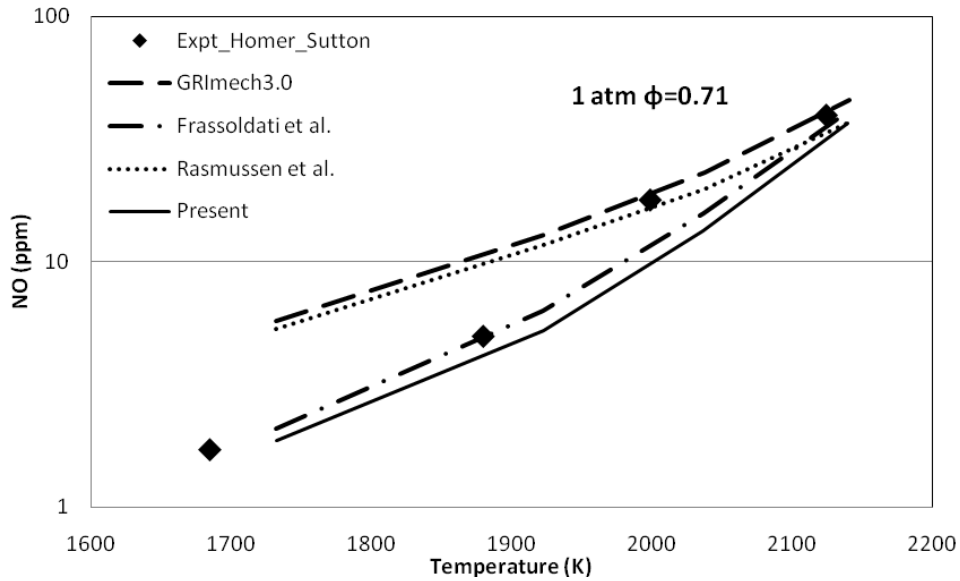


Fig 12: Measured (symbol) and calculated (lines) [NO] for 2 cm downstream of the flame front of flames of H₂ + O₂ + N₂. Equivalence ratio =0.71. Solid line: predicted [NO] using updated mechanism

Fig. 12 summarizes comparison of NO concentration at 2cm downstream of the flame front of H₂/O₂/N₂ flames from Homer and Sutton [72] at atmospheric pressure. The abscissa represents the adiabatic temperatures. Another interesting observation that can be drawn is that mechanism by Rasmussen et al [1] performs well for cases represented in fig 10 (O₂ % is increased to 21% and 23% in the O₂/N₂ mixture). As the O₂/N₂ ratio decreases (fig 11-12) , the mechanism[1] begin to deviate to a great extent. The present mechanism and that by Frassoldati et al.[9] seem to perform better. Hence, even under atmospheric pressure and lean conditions, certain mechanisms deviate for different mixture compositions.

Conclusion

- With thorough review of existing models that emerged in the last decade an updated kinetic mechanism is presented for Hydrogen combustion with NO_x prediction under conditions of high pressure (upto 20atm) and lean mixtures.
- Simulations using mechanisms by Rasmussen et al. [1], Frassoldati et al. [9], GRImech 3.0 [2] have been carried out and compared with the present updated mechanism.
- Mechanism by Rasmussen et al. [1] performs well under these conditions. At certain conditions of high N₂ in the oxidizer mixture(O₂/N₂) when the flame temperatures are low, present mechanism and that by Frassoldati et al.[9] perform better.
- GRImech 3.0 is not suitable for 100% H₂ high pressure and lean combustion.

Reference

- [1] Rasmussen C.L., Hansen J., Marshall P., Glarborg P., *Int J Chem Kinet*, 40:454-480(2008).
- [2] Gregory P. Smith, David M. Golden, Michael Frenklach, Nigel W. Morarty, Boris Eiteneer, Mikhail Goldenberg, C. Thomas Bowman, Ronald K. Hanson, Soonho Song, William C. Gardiner, Jr., Vitali V. Lissianski, and Zhiwei Qin, http://www.me.berkeley.edu/gri_mech/
- [3] Mueller M.A., Kim T.J., Yetter R.A., Dryer F.L., *Int J Chem Kinet* 31:113-125(1999).
- [4] Tsang, W. and Hampson, R. F. (1986) Chemical kinetic data base for combustion chemistry. Part I. Methane and related compounds. *J. Phys. Chem. Ref. Data*, 15: 1087.
- [5] Aung K.T., Hassan M.I., Faeth G.M., *Combust Flame*, 109: 1-24(1997).
- [6] Aung K.T., Hassan M.I., Faeth G.M., *Combust Flame*, 112: 1-15(1998).
- [7] Kim, T.J., Yetter, R.A., Dryer, F.L. (1994) *Twenty-Fifth Symposium (International) on Combustion*, The Combustion Institute, Pittsburgh, pp. 759-766.
- [8] Wang, W., and Rogg, B., *Combust. Flame* 94:271 (1993).
- [9] Frassoldati A., Faravelli T., Ranzi E., *Int J Hydrogen Energy*, 31:2310-2328(2006).
- [10] Tse S.D., Zhu D.L., Law C.K., *Proc. Combust Inst.*, 28:1793-1800(2000).
- [11] Taylor, S. C., Ph.D. Thesis, University of Leeds, 1991.
- [12] Kwon O.C., Faeth G.M., *Combust Flame*, 124:590-610(2001).
- [13] Wang B.L., Olivier H., Gronig H., *Combust Flame*, 133:93-106(2003).
- [14] D.L. Baulch, C.J. Cobos, R.A. Cox, P. Frank, G. Hayman, Th. Just, J.A. Kerr, T. Murrells, M.J. Pilling, J. Troe, R.W. Walker, J. Warnatz, *Combust. Flame*, 98 (1994) 59-79.
- [15] Allen M.T., Yetter R.A., Dryer F.L., *Int. J. Chem. Kinet.*, 27:883(1994).
- [16] Konnov A.A., Detailed reaction mechanism for small hydrocarbons combustion, Release 0.5, <http://homepages.vub.ac.be/~akonnov>
- [17] Miller J.A., Bowman C.T., *Prog. Energy Combust. Sci.* 15:287(1989).
- [18] Li J., Zhao Z., Kazakov A., Dryer F.L., *Int. J. Chem. Kinet.* 36: 566-575(2004).
- [19] Li J., Zhao Z., Kazakov A., Chaos M., Dryer F.L., et al. *Int J Chem Kinet* 39 (3): 109-136 (2007).
- [20] Skottene M., Rian K.E., *Int J Hydrogen Energy*, 32:3572-3585(2007).
- [21] Strohle J., Myhrvold T., *Int J Hydrogen Energy*, 144:545-557(2006).
- [22] Strohle J., Myhrvold T., *Int J Hydrogen Energy*, 32:125-135(2007).
- [23] Davis A.G., Joshi A.V., Wang H., Egolfopoulos F., *Proc. Combust. Inst.* 30 (2005) 1283-1292.
- [24] Saxena P., Williams F.A., *Combust. Flame* 145 (2006) 316-323.
- [25] Sun H., Yang S.I., Jomaas G., Law C.K., *Proc Combust Inst.* 31(2007)439-446.
- [26] Konnov A.A., *Combust Flame*, 152:507-528(2008).
- [27] Burke M.P., Chaos M., Dryer F.L., Ju Y., *Combust. Flame* 157 (2010) 618-631.
- [28] Glarborg P., Dam-Johansen K., Miller J.A., *Int J Chem Kinet.*, 27:1207-1220(1995).
- [29] Glarborg P., Alzueta A.U., Dam-Johansen K., Miller J.A., *Combust. Flame* 115:1-27 (1998).
- [30] Konnov A.A., Colson G., De Ruyck J., *Fuel*, 80:49-65(2001).
- [31] Konnov A.A., Dyakov I.V., De Ruyck J., *Proc. Combust Inst.* 29:2171-2177(2002).
- [32] Xie L., Hayashi S., Hirose K., *Twenty-Sixth Symposium(International) on Combustion/The Combustion Institute*, 2155-2160 (1996).
- [33] Harrington J.E., Smith G.P., Berg P.A., Noble A.R., Jeffries J.B., Crosley D.R., *Twenty-Sixth Symposium(International) on Combustion/The Combustion Institute*, 2133-2138 (1996).
- [34] Konnov A.A., De Ruyck J., *Combust. Sci and Technol.*, 152: 1, 23-37(2000).
- [35] Konnov A.A., De Ruyck J., *Combust. Flame*, 124: 106-126(2001).
- [36] Konnov A.A., De Ruyck J., *Combust. Sci and Technol.*, 168: 1, 1-46(2001).
- [37] Engleman V.S., Bartok W., Longwell J.P., Edelman R.B., *Fourteenth Symposium(International) on Combustion/The Combustion Institute*, 755-765 (1972).
- [38] Konnov A.A., *Combust. Flame*, 134: 421-424 (2003).
- [39] The San Diego Mechanism, [<http://maeweb.ucsd.edu/combustion/cermech/>]; 30 August, 2003
- [40] Bozzelli J.W., Dean A.M., *Int J Chem Kinet*, 27: 1097-1109(1995).

- [41] Xu S., Lin M.C., *Int J Chem Kinet*, 42:69-78(2010).
- [42] Xu S., Lin M.C., *Int J Chem Kinet*, 41:678-688(2009).
- [43] Xu S., Lin M.C., *Int J Chem Kinet*, 41:667-677(2009).
- [44] Frassoldati A., Faravelli T., Ranzi E., *Combust Flame*, 135:97-112(2003).
- [45] Konnov A.A., De Ruyck J., *Combust. Sci and Technol.*, 149: 53-78(1999).
- [46] Volkov E.N., Konnov A.A., Gula M., Holtappels K., Burluka A.A., *Proc. European Combustion Meeting*, 2009.
- [47] Shmakov A.G., Korobeinichev O.P., Rybitskaya I.V., Chernov A.A., Knyazkov D.A., Bolshova T.A., Konnov A.A., *Combust Flame*, 157:556-565(2010).
- [48] D.L. Baulch, C.J. Cobos, R.A. Cox, C. Esser, P. Frank, Th. Just, J.A. Kerr, M.J. Pilling, J. Troe, R.W. Walker and J. Warnatz, *J. Phys. Chem. Ref. Data* 21 (1992), p. 411.
- [49] Baulch D.L., Bowman C.T., Cobos C.J., Cox R.A., Just T., Kerr J.A., Pilling M.J., Stocker D., Troe J., Tsang W., Walker R.W., Warnatz J., *J. Phys. Chem. Ref. Data* 34 (3) (2005) 757-1397.
- [50] Miller J.A., Branch M.C., Kee R.J., *Combust Flame*, 43:81(1981).
- [51] O'Connaire M., Curran H.J., Simmie J.M., Pitz W.J., Westbrook C.K., *Int J Chem Kinet*, 36:603-622(2004).
- [52] Hwang S.M., Ryu S.O., De Witt K.J., Rabinowitz M.J., *Chemical Physics Letters*, 408:107-111(2005).
- [53] Troe V.G., Ushakov V.G., *J Chem. Phys.*, 115:3621(2001).
- [54] Cohen N., Westberg K.R., *J. Phys. Chem. Ref. Data*, 12: 531(1983).
- [55] Tsang, W. and Hampson, R. F., *J. Phys. Chem. Ref. Data*, 15: 1087. (1986).
- [56] Sutherland J.W., Michael J.V., Pirraglia A.N., *Proc. Combust. Inst.*, 21:929-941(1988).
- [57] Coppens, F.H.V., De Ruyck, J. Konnov, A.A., *Combust. Flame*, 149: 409-417 (2007)
- [58] Rohrig M., Wagner H.G., *Proc. Combust. Inst.* 25 (1994) 975-981.
- [59] Konnov A.A., *Combust. Flame*, 121:548-550(2000).
- [60] Konnov A.A., De Ruyck J., *Combust. Flame*, 125: 1258-1264(2001).
- [61] Park J., Giles N.D., Moore J., Lin M.C., *J Phys Chem A* 102:10099-10105(1998).
- [62] Glarborg P., Dam-Johansen K., Miller J.A., Kee R.J., Coltrin M.E., *Int J Chem Kinet.*, 26:421(1994).
- [63] R.J. Kee, F.M. Rupley, J.A. Miller, M.E. Coltrin, J.F. Grcar, E. Meeks, H.K. Moffat, A.E. Lutz, G. Dixon-Lewis, M.D. Smooke, J. Warnatz, G.H. Evans, R.S. Larson, R.E. Mitchell, L.R. Petzold, W.C. Reynolds, M. Caracotsios, W.E. Stewart, P. Glarborg, C. Wang, O. Adigun, Chemkin Collection, Release 3.6, Reaction Design, Inc., San Diego, CA, 2000.
- [64] Somers L.M.T., The simulation of flat flames with detailed and reduced chemical models, PhD. Thesis, Technische Universiteit Eindhoven (1994).
- [65] Burcat A., Ruscic B., "Third Millennium Ideal Gas and Condensed Phase Thermochemical Database for Combustion with updates from Active Thermochemical Tables" ANL-05/20 and TAE 960 Technion-IIT, Aerospace Engineering, and Argonne National Laboratory, Chemistry Division, September 2005.
- [66] Dowdy D.R., Smith D.B., Taylor S.C., *Proc. Combust. Inst.*, 23:325(1990).
- [67] Slack M.W., *Combust Flame*, 28:241-249 (1977).
- [68] Borisov A.A., Skachkov G.I., Oguryaev A.A., *Kinetics and Catalysis* 14 (1973) 294-300.
- [69] Javoy S., Mevel R., Paillard C.E., *Int J Chem Kinet*, 41:357-375(2009).
- [70] Sulzmann K.G.P., Kline J.M., Penner S.S., *Proc. Int. Symp.*, 12th, 1979, 465(1980).
- [71] Fujii N., Chiba K., Uchida S., Miyama H., *Chemical Physics Letters*, 127:2,141-144(1986)
- [72] Homer J.B., Sutton M.M., *Combust Flame* 20:71-76(1973).